Journal for ImmunoTherapy of Cancer

Multistep tumor genetic evolution and changes in immunogenicity trigger immune-mediated disease eradication in stage IV melanoma: lessons from a single case

Viviana Vallacchi ,[1] Elisabetta Vergani ,[1] Mara Cossa ,[2] Chiara Gargiuli ,[3] Adele Busico ,[4] Andrea Devecchi ,[4] Matteo Dugo ,[5] Laura Bergamaschi,[1] Loris De Cecco ,[6] Stefano Cavalieri ,[7,8] Barbara Valeri ,[2] Elena Tamborini ,[4] Gianfrancesco Gallino ,[9] Michele Del Vecchio ,[7] Mario Santinami ,[9] Marialuisa Sensi ,[3] Licia Rivoltini ,[1] Lorenza Di Guardo ,[7] Monica Rodolfo [1]

To cite: Vallacchi V, Vergani E, Cossa M, *et al*. Multistep tumor genetic evolution and changes in immunogenicity trigger immune-mediated disease eradication in stage IV melanoma: lessons from a single case. *Journal for ImmunoTherapy of Cancer* 2024;**12**:e007612. doi:10.1136/jitc-2023-007612

► Additional supplemental material is published online only. To view, please visit the journal online (http://dx.doi.org/10.1136/jitc-2023-007612).

VV and EV contributed equally.

VV and EV are joint first authors.

LDG and MR are joint senior authors.

Accepted 30 November 2023

For numbered affiliations see end of article.

Correspondence to
Dr Monica Rodolfo;
monica.rodolfo@istitutotumori.mi.it

ABSTRACT

Durable remissions are observed in 10%–20% of treated patients with advanced metastatic melanoma but the factors associated with long-term complete clinical responses are largely unknown. Here, we report the molecular characteristics of tumor evolution during disease progression along a 9-year clinical course in a patient with advanced disseminated melanoma who received different treatments, including trametinib, ipilimumab, radiation, vemurafenib, surgical tumor debulking and a second ipilimumab course, ultimately achieving complete long-term disease remission.

Longitudinal analyses of therapies-resistant metastatic tumors revealed the effects of different treatments on tumor's microenvironment and immunogenicity, ultimately creating a milieu favorable to immunotherapy response. Monitoring of the temporal dynamics of T cells by analysis of the T cell receptor (TCR) repertoire in the tumor and peripheral blood during disease evolution indicated that T-cell clones with common TCR rearrangements, present at low levels at baseline, were maintained and expanded after immunotherapy, and that TCR diversity increased. Analysis of genetic, molecular, and cellular components of the tumor depicted a multistep process in which treatment with kinase inhibitors strongly conditioned the immune microenvironment creating an inflamed milieu converting cold into hot tumors, while ipilimumab impacted and increased the TCR repertoire, a requirement for tumor rejection.

Since the optimal sequencing of treatment with antibodies targeting immune checkpoints and kinase inhibitors for advanced melanoma is still clinically debated, this case indicates that immunotherapy success is possible even after progression on targeted therapy.

INTRODUCTION

In advanced melanoma, complete responses to treatment are restricted to a small fraction of patients due to acquired or primary resistance to therapy. In the case of immune checkpoint inhibitors (ICIs), the molecular factors determining the response of the tumor and host remain elusive.[1] Genomic analysis of longitudinal tumor samples is a way to obtain information about tumor evolution and the effects of therapies on the composition of the tumor microenvironment (TME). The genetic evolution of melanoma in long-term survivors identified distinct poorly immunogenic melanoma phenotypes evolving after long-term latency.[2] Tumor phylogeny studies revealed that dysregulation of genomic integrity and large-scale copy number alterations (CNAs) dominate disease progression.[3 4] Transcriptomic analysis of longitudinal tumor biopsies collected during treatment showed that the early activation of the adaptive immune response can be predictive of response to immunotherapy with ICIs[5] and that increased richness of T cell receptor (TCR) diversity in peripheral blood and in tumor-infiltrating lymphocytes (TILs) after ICI treatment could associate with clinical benefit.[6–8]

RESULTS

The patient's clinical course and follow-up shown in figure 1 provided longitudinal samples for the characterization of tumor genomic profiles, tumor immune microenvironment (TIME) factors, and TCR repertoires associated with therapy resistance and treatment response. Due to the early times

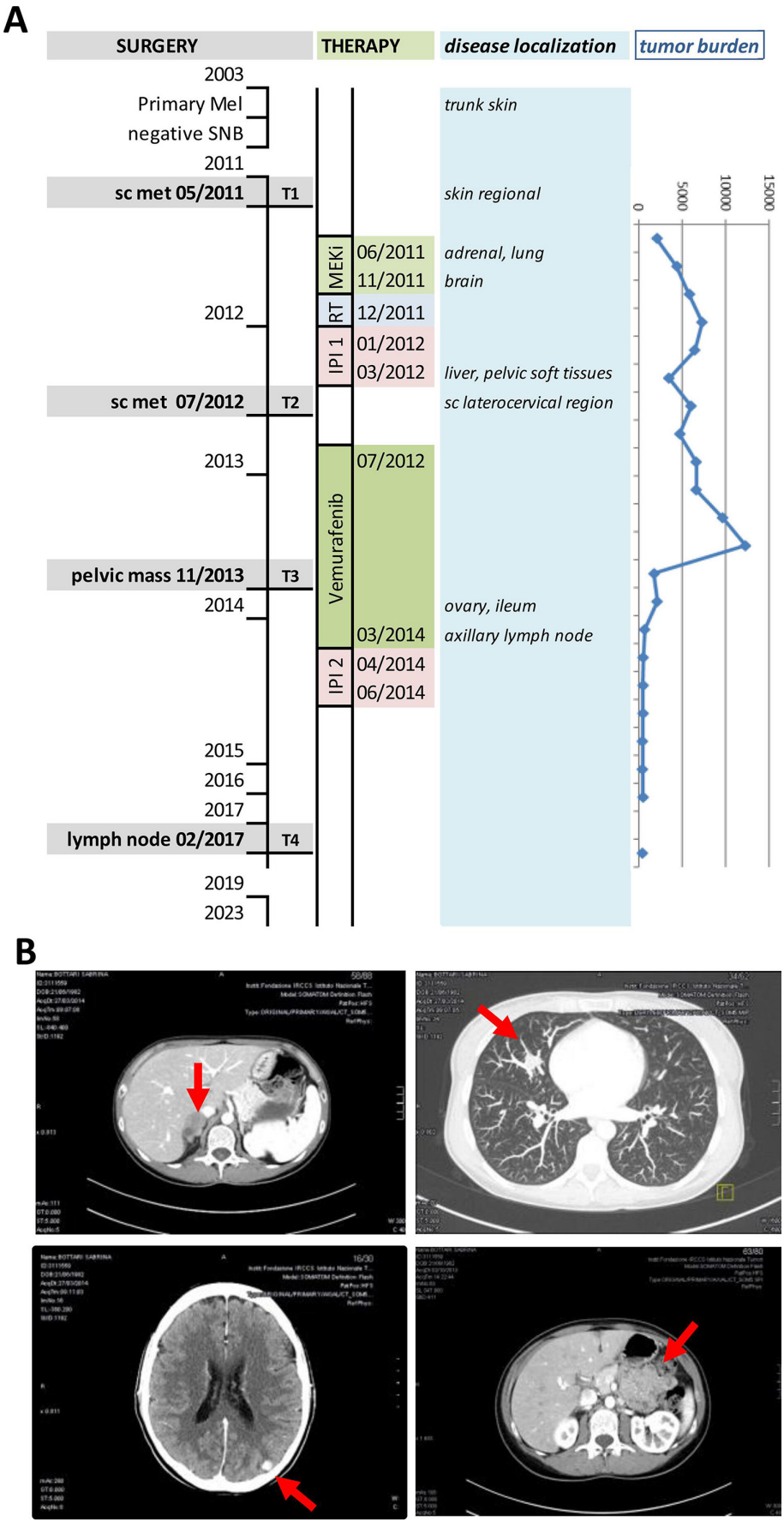

Figure 1 (Continued)

Figure 1 (A) Clinical history of the patient, course of treatments and samples timing. In 2011, the patient was in late 20s when presented with a dermal melanoma lesion that was excised (tumor sample T1). The primary tumor was removed 8 years before when the patient was staged as pT2bN0M0 stage IIA. CT scan showed metastases in the right adrenal gland and two lung lesions, and since the T1 tumor was BRAF-V600E mutated, the patient was enrolled in a phase III clinical trial comparing trametinib with chemotherapy (trial MEK114267). The patient was randomized to receive trametinib and underwent 5 months of treatment (June–November 2011), until lung and adrenal disease progression and new brain metastasis were detected. The patient was given whole brain radiotherapy (total 30 Gy), and four courses of ipilimumab (3 mg/kg every 21 days) from January to March 2012 (IPI1) through an expanded-access program. After a partial response, 6 months later the disease progressed in the brain, lung, adrenal, liver, and pelvic soft tissues. BRAF mutation was confirmed in a cutaneous metastasis (tumor sample T2), and vemurafenib (1920 mg/24 hours) was started in September 2012 in an expanded-access program. CT scans showed partial reduction of brain, lung, and adrenal metastases and stable disease in liver and soft tissues, until pelvic disease progression occurred (October 2013). An explorative laparotomy evidenced a large pelvic mass (tumor sample T3) infiltrating the left ovary (tumor sample T3A) and meso-sigma (tumor sample T3B), which was totally removed (November 2013). Three months later, as the disease in the lungs, right adrenal gland, and right axillary lymph nodes progressed, an immunotherapy rechallenge with ipilimumab was offered. The patient received re-induction with ipilimumab with the same dosage and schedule from April to June 2014 (IPI2) in an expanded-access program, and a partial response in all sites of disease was detected 1 month after the end of treatment. The toxicities included diffuse vitiligo (which persisted) and asymptomatic Graves' disease-related thyrotoxicosis (which resolved without treatment). Regular follow-up CT scans evidenced continuous tumor shrinkage in all disease locations. The patient remained tumor-free until February 2017, when an axillary lymph node became clinically evident, and complete lymph node dissection was performed, revealing one node out of 26 examined with tumor involvement (tumor sample T4). The patient received no subsequent treatment and at the time of this report (March 2023) remains free of disease. Tumor burden is calculated by the sum of the volumetric measurements based on the CT scans. Sc met, subcutaneous metastasis. (B) CT scan images: March 2013 adrenal, lung, and brain lesions; October 2013 pelvic mass; lesions are indicated by arrows.

in kinase inhibitors and ICI usage, this case offered the unique opportunity to investigate how different single treatments impact tumor genetics and local and systemic immunity.

To explore the effect of treatment on tumor genomic evolution, tumor samples T1–T4 (figure 1) obtained from four different surgeries, were analyzed for their genetic and transcriptional profiles. Whole genome CNA and targeted mutation analyses showed evidence of a clonal pattern of disease progression as individual CNAs and point mutations were detected in addition to a set of common genetic aberrations (figure 2A–B, online supplemental table S1). All lesions showed mutations in the *BRAF* and *ATRX* genes and *TERT* promoter, while individual mutations in *GATA3* (T2), *FBXW7* and *MAP2K1* genes (T3), and *NRAS* genes (T4) were detected, all possibly associated with BRAF inhibitors (BRAFi) resistance. Consistently, the cell line SB derived from the T4 tumor specimen showed an identical profile, with *BRAF*, *ATRX*, and *RAS* alterations and in vitro resistance to BRAFi[9] (online supplemental figure S1A). These results indicate that tumor genetic evolution was shaped by treatment with the BRAFi, which led to the selection of melanoma subpopulations carrying mutations related to acquired BRAFi resistance.

At the transcriptional level, single-sample gene set enrichment analysis (ssGSEA) revealed that tumors were characterized by unique patterns of enrichments included in the *signal transduction* and *immune system* Reactome categories (online supplemental table S2), indicating that a remarkable reshaping of signaling pathways and the immune response at the tumor level associated with tumor progression. *Immune system* category showed a significant positive enrichment of non-overlapping signatures linked to both *adaptive immunity* and *innate immunity* only in T3B and T4 (figure 2C). The signatures enriched in T3B suggested a highly inflamed TIME with some signs of adaptive responses, while in T4, the inflammatory signatures were less enriched, and specific T-cell signatures were displayed. Such a pattern was confirmed by the high protein levels of the inflammatory factors CXCL8 and CXCL7 in T3 tumor tissue lysate, and of CCL5 and CXCL10, which are mainly produced by adaptive immune responses, in T4 (data not shown). Consistently, cellular deconvolution analysis revealed enrichment of T central memory, T naïve, activated CD4, T helper 2, and gdT cells in T3B, while T4 showed enrichment of cytotoxic CD8, T effector memory, CD4 T regulatory, T helper-follicular, and exhausted lymphocyte populations. Notably, T3B showed enrichment of myeloid-derived suppressor cells (MDSCs) while T4 showed enrichment of M1 and M2 macrophages and activated dendritic cells (figure 2D).

Tissue immunostaining confirmed a prevalent lack of intratumoral T-cell markers in T1, with positive staining for CD3 found only in the tumor margin, while staining for the macrophage marker CD68 was intense. The other samples displayed a gradual increase in intratumor infiltrating cells positive for CD3, CD8, CD4, and for programmed cell death 1 (PD-1) T-cell activation marker (figure 3A–B). In agreement with the specific enrichment of the *interferon-gamma (IFNγ) signaling* gene signature, T4 was the only sample that showed positive programmed death ligand 1 (PDL-1) staining (figure 3C). Indeed, the expression of PDL-1 could be induced in the T4-derived cell line SB by IFNγ treatment, suggesting that IFNγ was produced in the TME (online supplemental figure S1B–C). In-depth characterization of the composition of the T-cell compartment in the T4 nodal metastasis confirmed the relevance of regulatory and activated/exhausted populations (online

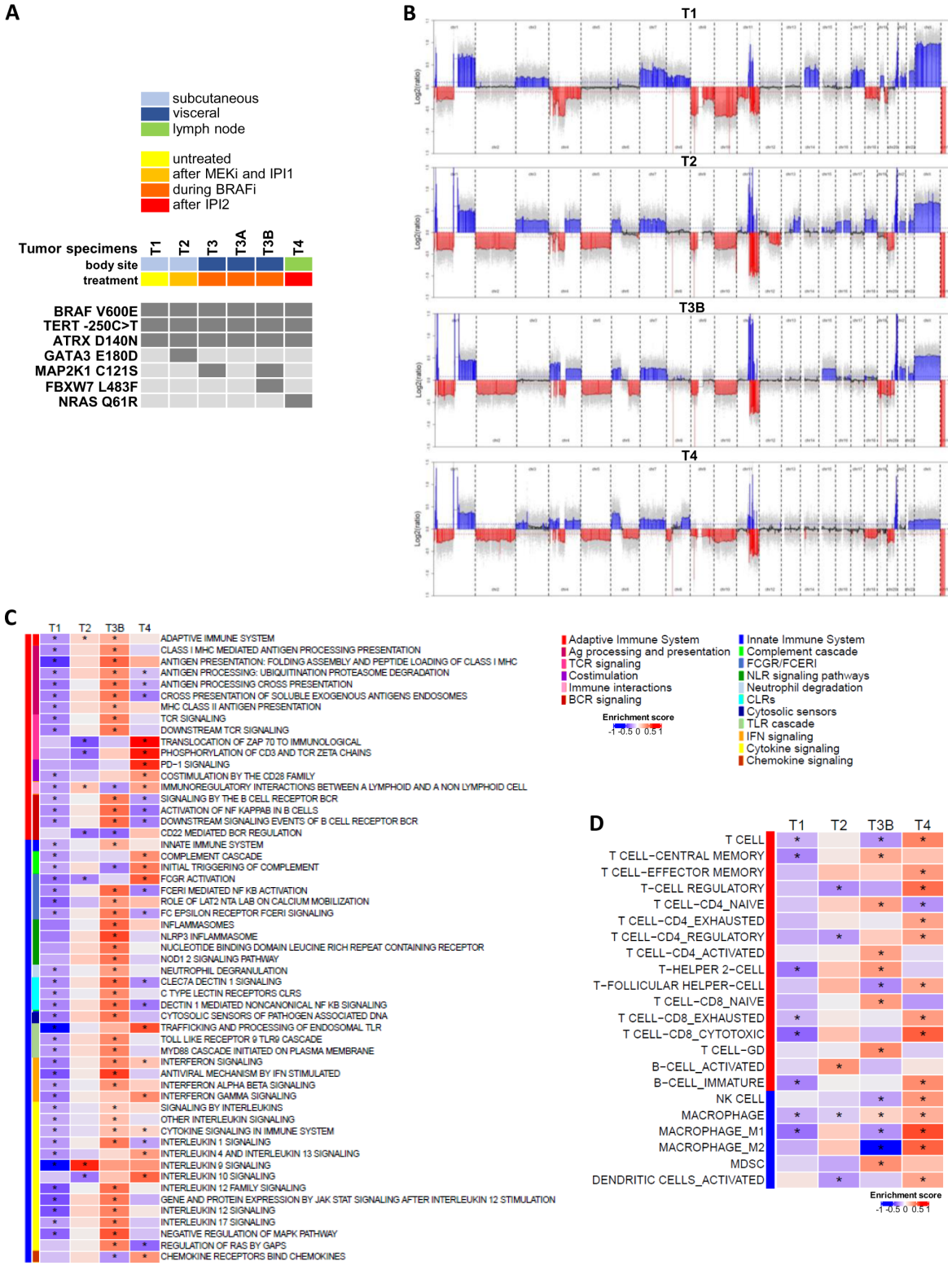

Figure 2 Genetic and transcriptional profiles of T1–T4 tumor samples. (A) Pathogenic gene variants detected by targeted mutation analysis performed by the Ion Torrent Personal Genome platform (ThermoFisher Scientific). (B) Copy number alteration (CNA) genomic plots obtained by analysis by OncoScan CNV arrays (Affymetrix). The figure displays the log R ratio, the x-axis represents the chromosomes. T3 samples were obtained from the pelvic mass, and T3A was localized in the ovary while T3B in the ileum. (C) Heatmap of enriched Reactome gene sets for Immune genes in individual T1–T4 transcriptional profiles as resulting from single-sample gene set enrichment analysis (ssGSEA) of transcriptional profiles obtained by Affymetrix ClariomS GeneChip Assay (Affimetrix). Significant enrichments ($p<0.01$) are indicated by an asterisk. (D) Immune cells deconvolution analysis. Immune cells gene signatures used for deconvolution are reported in online supplemental methods table 1. The red section includes genes sets of immune cell populations relative to *adaptive immunity*, while the blue section includes those relative to *innate immunity*.

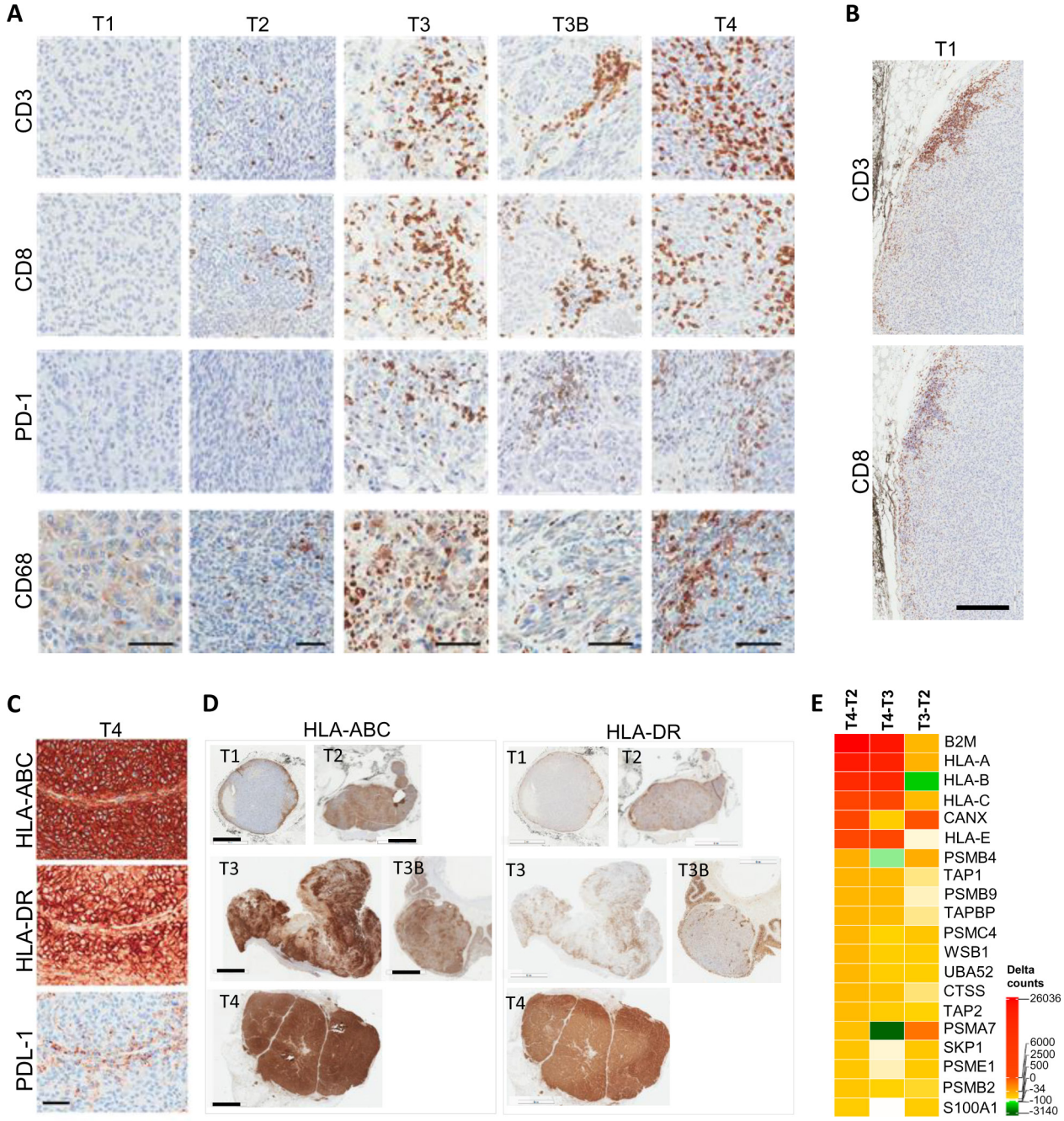

Figure 3 Tumor immune microenvironment (TIME) profiles of T1–T4 tumor samples. (A) Tumor immunostaining for tumor-infiltrating immune cells (bar 100 µm). (B) Spots of T cells accumulation at the tumor border in T1 sample. Bar 200 µm. (C) Immunostaining for programmed death ligand 1 (PDL-1) in T4 sample (bar 50 µm). (D) Snapshots of T1–T4 tumor sections stained with HLA-ABC and HLA-DR antibody (bar 3 mm). All samples stained positive for S100, HMB45, SOX1 melanoma markers (not shown). (E) Heatmap showing upregulation of molecules involved in major histocompatibility complex (MHC) class I-mediated antigen processing and presentation machinery in T2, T3, and T4. The top 20 genes upregulated in T4 compared with T2 are shown; HLA-A, HLA-B, HLA-C, HLA-E, and B2M, as well as other molecules involved in antigen presentation (CANX, TAP1, TAPBP, and TAP2) and in antigen processing (PSMB4, PSMB9, PSMC4, WSB1, UBA52, PSMA7, SKP1, PSME1, and PSMB2) are included.

supplemental figure S2). Interestingly, T1 stained negative for human leukocyte antigen (HLA) class I, while T2 showed some positivity in melanoma cells, and T3B and T4 displayed strong staining, indicating that upregulation of antigen-presenting molecules could underlie the increase in T-cell infiltration and activity. T3B and particularly T4 sample also displayed HLA class II positivity (figure 3D). A consistent and concomitant upregulation of molecules involved in major histocompatibility complex (MHC) class I-mediated antigen processing and presentation from T2 to T4 was confirmed also at transcriptional level (figure 3E).

To gain insights into the temporal dynamics of T cells during the disease course at the local and systemic levels, the TCR-beta (TCRB) chain repertoire was assessed by ImmunoSEQ (Adaptive Technologies) in T1–T4 tumor samples, in one regional tumor-free lymph node (LN1) obtained at the T4 surgery, and in peripheral blood obtained at three different time points (the first (WB1, March 2012) between the T1 and T2 surgeries and after the last ipilimumab infusion, the second (WB2, February 2017) obtained at T4-LN1 surgery, and the last (WB3, January 2019) obtained at disease remission 2 years later). At difference with sampling for transcriptomic analysis for which the tissue section areas were selected for high tumor cellularity, for this analysis the T cell-rich peritumoral tissue margin of T1 was included. The analysis of productive TCRB rearrangements, at amino acid level, identified a large degree of similarity between T1 (excised before any treatment) and T2 (excised 1 year later, after treatment with MEK and IPI1), while T3B and T4 showed different patterns (figure 4A, online supplemental figure S3A–B). TCR rearrangements intersection revealed that TILs enriched at the T1 border persisted in the circulation (WB1) and infiltrated the T2 tumor. Similarly, WB2, the T4-synchronous blood sample, showed T-cell clones that had accumulated in LN1 non-invaded LN from the same basin and were also present in T4 TILs (figure 4B). TCRB rearrangements were shared by all blood samples, up to 2 years after T4 excision (online supplemental figure S3C). Longitudinal tracking of representative clonotypes showing a productive frequency >0.1% (online supplemental table S3) identified some of them which, present at low frequency in baseline T1 tumor, had expanded or persisted in all the other specimens during therapy. Others instead, present in T1 or shared between T1 and T2, decreased in all other specimens and were mostly undetected or present at low frequency in blood. Increase of clonotypes only at specific tumor sites was also observed (figure 4C). TCR diversity in tumor specimens increased during the disease course, as shown by the decrease in clonality, and the same trend was observed in blood (figure 4D). Consistently, a decrease during treatment was observed for the frequency of the most abundant clone after computationally down-sampling, as per cent maximal productive frequency (figure 4D), as well as for the total productive frequencies of the top 20 TCRB rearrangements of each sample (online supplemental figure S3B), indicating that the frequency of bioidentical TCRB clonotypes drops in blood and tumor lesions at therapy response, and a more diverse TCR repertoire is detected.

The matching of the identified complementarity-determining regions (CDRs) in the public database *VDJdb* identified a list of identical TCR clonotypes, which included specificity for the melanoma-associated antigen MAGEA6 and NRAS epitopes within the patient's specific HLA molecules (haplotype HLA-A*01),[10 11] for Melan-A melanoma antigen (ELAGIGILTV peptide) and for other tumor-associated antigens (TAAs) in HLA-A*02 haplotype (online supplemental table S4). The presence of IFNγ-producing $CD8^+$ T cells upon recognition of Melan-A peptides by lymphocytes obtained from peripheral blood mononuclear cells banked in 2019 (WB3) was detectable by flow cytometry (figure 4E).

DISCUSSION

Ipilimumab, a first-in-class ICI antibody, increased long-term survival in patients with advanced melanoma in phase II and III clinical trials.[12] After anti-PD-1 antibodies, which show superior first-line efficacy, ipilimumab is used only in selected cases. Few patients show dramatic responses to ipilimumab, making cytotoxic T-lymphocyte associated protein 4 (CTLA-4) an important immunotherapy target. Trials to determine the most active regimen and sequence of ICIs and targeted therapy for patients with advanced BRAF-mutant melanoma so far favored an initial dual ICI combination over a treatment sequence beginning with BRAFi/MEKi.[13 14] In addition, retrospective analysis of clinical results from a real-world setting revealed that a very low proportion of patients progressing on targeted therapy went on to receive a second-line ICI due to rapid disease progression.[15] Although the current practice does not include the single treatments given to this patient, nonetheless this case indicates that immunotherapy rechallenge after targeted therapy in combination with surgical debulking can be effective, and that acquired resistance to ICIs in melanoma can be reversed, with resistant tumors potentially showing a response to therapy rechallenge.[16 17] Even though it is not clear how commonly this change may occur, this particular case clearly shows that kinase inhibitors strongly regulated the TIME and tumor evolution from an immunologically cold to a hot tumor, thereby augmenting the effectiveness of immunotherapy, as previously shown for targeted therapy and for some other types of therapy.

This clinical case offered the exceptional opportunity to analyze metastatic tumors resistant to different treatments that were obtained at disease progression despite MEKi treatment and IPI1 (T2), vemurafenib (T3), and IPI2 (T4) and compare them with a baseline untreated tumor (T1). Interestingly, the results show that the induction of an immune-permissive microenvironment occurred as a multistep process, and immunogenicity determinants were progressively acquired to eventually achieve tumor rejection. As such, we can imagine T1 recurrence as the result of a tumor immunoediting process that promoted immune evasion in the presence of an active antitumor T-cell response during the 8 years of tumor dormancy that occurred after the primary tumor excision. The peculiarity of T1 is the lack of HLA class I expression and the *immune-cold* TIME, despite the clonality of T lymphocytes accumulating peritumorally and in blood detected by TCRB analysis. At transcriptional level, HLA class I and B2M transcripts were detectable, although expressed at low levels along with reduced expression of genes involved in antigen-presenting and antigen-processing machinery.

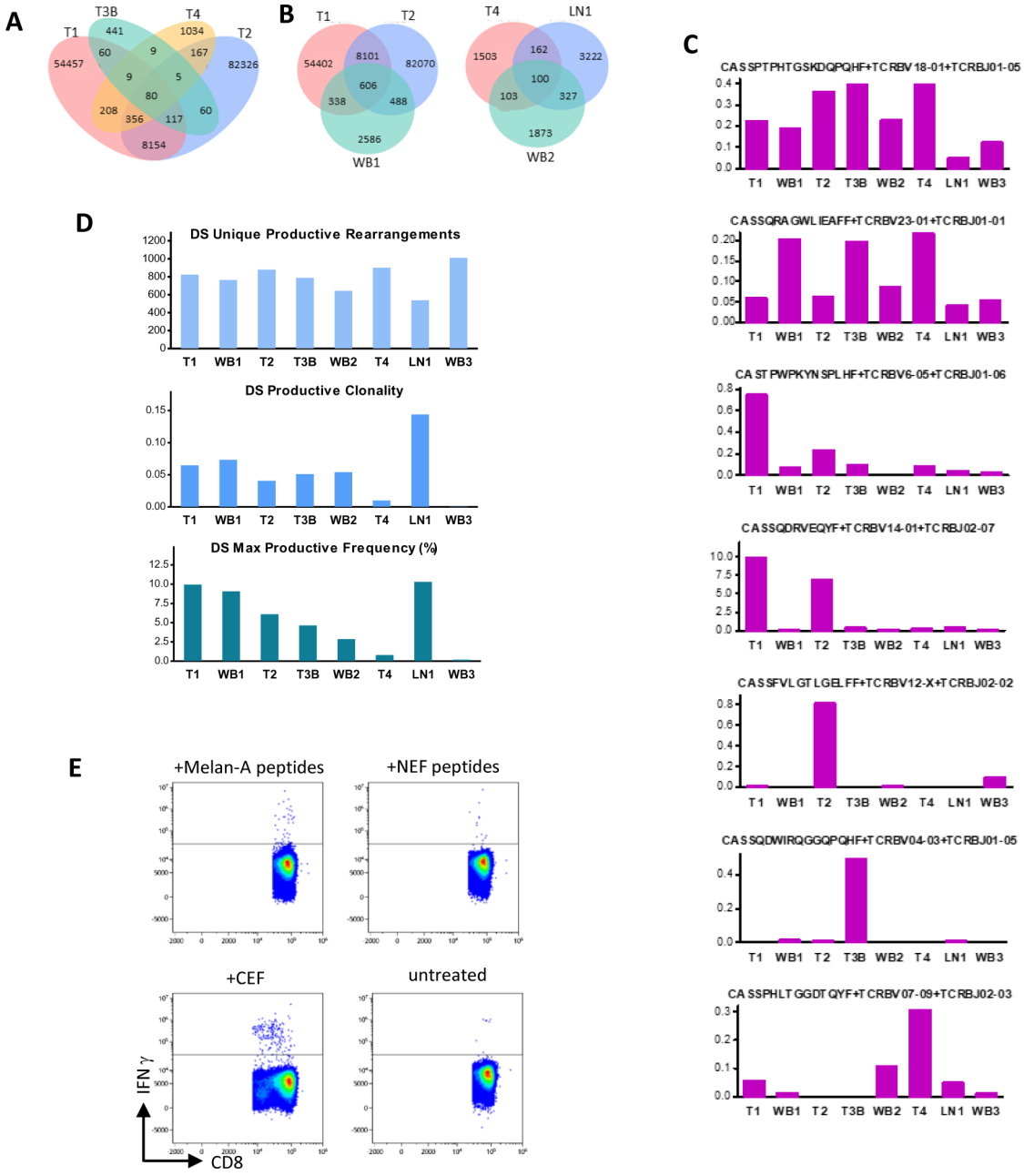

Figure 4 Longitudinal analysis of the T cell receptor-beta (TCRB) repertoire in tumor samples and the circulation reveals early expansion of common clones and an increase in clonotypes during treatment. (A) Venn diagrams displaying common TCR AA rearrangements in T1–T4 tumor samples and (B) in T1, WB1, and T2 (left), and in the synchronous T4, LN1, and WB2 samples (right). (C) Longitudinal TCR clonotype analysis in tumor, blood, and regional lymph node tissues. Representative clonotypes expanding in all specimens, enriched in T1 and T2, and clonotypes absent or present at low frequency at baseline and showing high frequency at specific tumor sites. (D) Top: TCR repertoire diversity, as numbers of unique productive TCR rearrangements in the different samples after normalization with down-sampling (DS). Middle: distribution spectrum of TCR clones, as productive clonality evenness index. Value of 1 indicate a monoclonal population. Bottom: frequency of the most abundant clones in every sample, as per cent maximal productive frequency. (E) Flow cytometry detection of Melan-A-specific CD8 T cells in peripheral blood mononuclear cell (PBMC) from peripheral blood banked in 2019 (WB3) on stimulation with synthetic peptides. Positivity of intracellular interferon-gamma (IFNγ) in $CD3^{+}CD8^{+}$ lymphocytes after stimulation with Melan-A is 0.029% (42/140,827), with positive control CEF is 0.198% (193/97,193), after negative control HIV-1 NEF peptide pool is 0.010% (12/115,275), while in non-stimulated lymphocytes staining is 0.008% (10/120,564).

It is not possible to precisely determine whether the type of alteration underlying the lack of HLA-I expression in T1 might have resulted from epigenetic silencing induced by cancer immunoediting mechanisms, as described,[18] or by genetic events occurring in upstream regulatory genes in tumor lesions. The loss of these genes appears unlikely as CNA analysis did not show alterations in chromosomal regions where MHC and B2M genes are localized.

Mechanisms underlying upregulation of the expression of molecules involved in MHC class I antigen processing and presentation during disease progression remain to be investigated. Remarkably, subsequent therapy with a MEKi and then with IPI1 led to a treatment-resistant tumor (T2) that expressed HLA-I, in line with the ability of MEKis to increase MHC class I and TAA presentation in melanoma cells.[19] The acquisition of HLA class I expression represents a step towards an immune-vulnerable state of the tumor, as reduction or loss of MHC class I protein expression is a common mechanism of tumor immune evasion associated with poor clinical outcomes in melanoma and other tumor types. As well, alterations in the expression of MHC class II have long been reported in melanoma, often in relation to metastatic progression, immune evasion, and clinical outcome. High levels of HLA class II gene expression were previously found to be associated with high T-cell infiltration, and therapeutic response to ICIs.[20 21] In line with this, T4 showed the features of an ICI-responsive tumor even though it was derived from tumor cells resistant to IPI2. In particular, the high level of PD-1$^+$ T cells suggests potential responsiveness to treatment with anti-PD-1 immunotherapy.

Surgical debulking of the large pelvic tumor mass that progressed during BRAFi treatment (T3) may have played a role in the multistep acquisition of immunogenic properties. Although metastatic progression following surgical tumor resection is often observed as a consequence of cancer cell shedding into the circulation and stimulation of angiogenesis, it is also well known that reduced tumor burden can impact immunological control of cancer, as tissue damage provoked by surgical stress can cause activation of both innate and adaptive immune responses. Several studies in murine models have implicated the myeloid cell remodeling induced by systemic wound healing programs by showing that tumor resection causes the removal of MDSCs from the TME and circulation, resulting in the activation of effector T cells and ultimately restoring systemic immune capacity for strong adaptive responses.[22 23] In addition, reducing the tumor load may allow T cells to target a few specific lesions. In this setting, although CD68 tissue staining for myeloid cells did not evidence major quantitative differences in T3 and T4, immune deconvolution analysis of transcriptional profiles is suggestive of a change of infiltrating myeloid cells.

At baseline and during treatment, TILs and circulating T cells contained a low but reproducible frequency of rearrangements of CDR3 and even TCR bioidentity to clonotypes recognizing Melan-A without shared HLA class I restriction. This finding supports the existence of shared clonotypes across individuals with the same cancer type, as reported for melanoma[24] and patients with other tumors.[25 26] Although the patient's reactivity against Melan-A was detectable, the specificity of the identified common TCRs remains to be established. The presence of CDR3 motifs and TCRB clonotypes identical to those specific for TAA restricted to mismatched HLA alleles was a common feature of TILs as also shown in a cohort of pretherapy lesions from patients with metastatic BRAF-mutated melanoma (data not shown). Whether the patient's TCR clonotypes include neoantigen specificity remains to be studied. Overall, TCR clonality decreased as TCR diversity increased during the treatment course in TILs as well as in the periphery, indicating that an increase in the TCR repertoire might associated with ICI response, as formerly reported,[6–8] and supporting the hypothesis that dynamic changes in the TCR repertoire are a clinical parameter for monitoring treatment responses.

Author affiliations
[1]Department of Experimental Oncology, Unit of Translational Immunology, Fondazione IRCCS Istituto Nazionale dei Tumori, Milan, Italy
[2]Pathology Department, Fondazione IRCCS Istituto Nazionale dei Tumori, Milan, Italy
[3]Applied Research and Technology Development Department, Fondazione IRCCS Istituto Nazionale dei Tumori, Milan, Italy
[4]Department of Diagnostic Innovation, Fondazione IRCCS Istituto Nazionale dei Tumori, Milan, Italy
[5]Department of Medical Oncology, San Raffaele Hospital, Milan, Italy
[6]Integrated Biology of Rare Tumors, Fondazione IRCCS Istituto Nazionale dei Tumori, Milan, Italy
[7]Medical Oncology, Fondazione IRCCS Istituto Nazionale dei Tumori, Milan, Italy
[8]Department of Oncology and Hemato-oncology, University of Milan, Milan, Italy
[9]Melanoma Surgery, Fondazione IRCCS Istituto Nazionale dei Tumori, Milan, Italy

Acknowledgements We acknowledge the excellent skills and technical contribution of Paola Squarcina, Simona Frigerio, Paola Deho, Eriomina Shahaj, Martina Filugelli, and Edoardo Marchesi. We thank the Pathology Tissue Bank and Antonia Martinetti (Medical Oncology Unit) for providing samples, Barbara Vergani (University of Milano Bicocca) for tissue imaging. We acknowledge Adaptive Biotechnology Young Investigators Awards to Eriomina Shahaj and Matteo Dugo. We acknowledge Springer Nature Author Services for English editing.

Contributors MR, MSe, and LDG designed the study. LDC, MD, ET, and CG developed methodology. Research was performed by MC, AB, AD, and LB. Data were analyzed by BV, SC, GG, MDV, MSa, and LR. VV, EV, MSe, and MR wrote the manuscript with input from all coauthors. LDG, LR, VV, and EV edited the manuscript. MR is guarantor for this work.

Funding Ministero della Salute: RCR2020 to ACC Melanoma Working Group, and Ricerca Corrente; AIRC IG17462; CARIPLO Foundation (2015-0911, VV support).

Competing interests None declared.

Patient consent for publication Consent obtained directly from patient(s).

Ethics approval Blood and tumor samples were obtained on signed informed consent to the study according to protocols approved by the IRB of Fondazione IRCCS Istituto Nazionale dei Tumori and the Independent Ethics Committee approved the study protocols INT40/11 and INT91/17. Participants gave informed consent to participate in the study before taking part.

Provenance and peer review Not commissioned; externally peer reviewed.

Data availability statement The gene expression dataset of tumor samples is deposited in Gene Expression Omnibus with accession number GSE171484. TCRB datasets have been deposited and will be available at Adaptive ImmuneACCESS database on registration. The cell line SB is available on request.

ORCID iDs
Viviana Vallacchi http://orcid.org/0000-0002-2819-0630
Elisabetta Vergani http://orcid.org/0000-0001-6689-4981
Mara Cossa http://orcid.org/0000-0002-0697-3431
Chiara Gargiuli http://orcid.org/0000-0002-6973-9634
Adele Busico http://orcid.org/0000-0002-5808-0387
Andrea Devecchi http://orcid.org/0000-0003-0440-3221
Matteo Dugo http://orcid.org/0000-0001-9786-2763
Loris De Cecco http://orcid.org/0000-0002-7066-473X
Stefano Cavalieri http://orcid.org/0000-0003-1294-6859
Barbara Valeri http://orcid.org/0000-0001-9143-7280
Elena Tamborini http://orcid.org/0000-0002-3819-8687
Gianfrancesco Gallino http://orcid.org/0000-0001-6639-1815
Michele Del Vecchio http://orcid.org/0000-0001-9060-2512
Mario Santinami http://orcid.org/0000-0001-8436-4757
Marialuisa Sensi http://orcid.org/0000-0002-7643-0248
Licia Rivoltini http://orcid.org/0000-0002-2409-6225
Lorenza Di Guardo http://orcid.org/0000-0002-7297-319X
Monica Rodolfo http://orcid.org/0000-0002-9196-0298

REFERENCES

1 Karasarides M, Cogdill AP, Robbins PB, *et al*. Hallmarks of resistance to immune-checkpoint inhibitors. *Cancer Immunol Res* 2022;10:372–83.
2 Zhao F, Sucker A, Horn S, *et al*. Melanoma lesions independently acquire T-cell resistance during metastatic latency. *Cancer Res* 2016;76:4347–58.
3 Harbst K, Lauss M, Cirenajwis H, *et al*. Molecular and genetic diversity in the metastatic process of melanoma. *J Pathol* 2014;233:39–50.
4 Vergara IA, Mintoff CP, Sandhu S, *et al*. Evolution of late-stage metastatic melanoma is dominated by aneuploidy and whole genome doubling. *Nat Commun* 2021;12:1434.
5 Chen P-L, Roh W, Reuben A, *et al*. Analysis of immune signatures in longitudinal tumor samples yields insight into biomarkers of response and mechanisms of resistance to immune checkpoint blockade. *Cancer Discov* 2016;6:827–37.
6 Postow MA, Manuel M, Wong P, *et al*. Peripheral T cell receptor diversity is associated with clinical outcomes following Ipilimumab treatment in metastatic melanoma. *J Immunother Cancer* 2015;3:23.
7 Valpione S, Mundra PA, Galvani E, *et al*. The T cell receptor repertoire of tumor infiltrating T cells is predictive and Prognostic for cancer survival. *Nat Commun* 2021;12:4098.
8 Robert L, Tsoi J, Wang X, *et al*. Ctla4 blockade broadens the peripheral T-cell receptor repertoire. *Clin Cancer Res* 2014;20:2424–32.
9 Vergani E, Busico A, Dugo M, *et al*. Genetic layout of melanoma lesions is associated with BRAF/MEK-targeted therapy resistance and transcriptional profiles. *J Invest Dermatol* 2022;142:3030–40.
10 Gros A, Parkhurst MR, Tran E, *et al*. Prospective identification of neoantigen-specific lymphocytes in the peripheral blood of melanoma patients. *Nat Med* 2016;22:433–8.
11 Peri A, Greenstein E, Alon M, *et al*. Combined presentation and Immunogenicity analysis reveals a recurrent RAS.Q61K Neoantigen in Melanoma. *J Clin Invest* 2021;131:e129466.
12 Hodi FS, O'Day SJ, McDermott DF, *et al*. Improved survival with Ipilimumab in patients with metastatic melanoma. *N Engl J Med* 2010;363:711–23.
13 Atkins MB, Lee SJ, Chmielowski B, *et al*. Combination dabrafenib and trametinib versus combination nivolumab and Ipilimumab for patients with advanced *BRAF*-mutant melanoma: the dreamseq trial-ECOG-ACRIN Ea6134. *J Clin Oncol* 2023;41:186–97.
14 Ascierto PA, Mandalà M, Ferrucci PF, *et al*. Sequencing of Ipilimumab plus nivolumab and encorafenib plus Binimetinib for untreated *BRAF*-mutated metastatic melanoma (SECOMBIT): a randomized, three-arm, open-label phase II trial. *J Clin Oncol* 2023;41:212–21.
15 Jones J, Lucey R, Corrie P. Retrospective review of outcomes associated with metastatic melanoma patients treated with 1ST-line BRAF-targeted therapy. *Pigment Cell Melanoma Res* 2022;35:595–604.
16 Kato J, Hida T, Kamiya T, *et al*. Rechallenge with nivolumab after vemurafenib treatment of initially Nivolumab-resistant advanced Melanoma. *JAMA Dermatol* 2018;154:621–2.
17 Schoenfeld AJ, Hellmann MD. Acquired resistance to immune checkpoint inhibitors. *Cancer Cell* 2020;37:443–55.
18 Aptsiauri N, Garrido F. The challenges of HLA class I loss in cancer Immunotherapy: facts and hopes. *Clin Cancer Res* 2022;28:5021–9.
19 Stopfer LE, Rettko NJ, Leddy O, *et al*. MEK inhibition enhances presentation of targetable MHC-I tumor antigens in mutant melanomas. *Proc Natl Acad Sci USA* 2022;119:e2208900119.
20 Rodig SJ, Gusenleitner D, Jackson DG, *et al*. MHC proteins confer differential sensitivity to CTLA-4 and PD-1 blockade in untreated metastatic melanoma. *Sci Transl Med* 2018;10:eaar3342.
21 Johnson DB, Estrada MV, Salgado R, *et al*. Melanoma-specific MHC-II expression represents a tumour-autonomous phenotype and predicts response to anti-PD-1/PD-L1 therapy. *Nat Commun* 2016;7:10582.
22 Danna EA, Sinha P, Gilbert M, *et al*. Surgical removal of primary tumor reverses tumor-induced immunosuppression despite the presence of metastatic disease. *Cancer Res* 2004;64:2205–11.
23 Allen BM, Hiam KJ, Burnett CE, *et al*. Systemic dysfunction and plasticity of the immune macroenvironment in cancer models. *Nat Med* 2020;26:1125–34.
24 Huuhtanen J, Chen L, Jokinen E, *et al*. Evolution and modulation of antigen-specific T cell responses in melanoma patients. *Nat Commun* 2022;13:5988.
25 Munson DJ, Egelston CA, Chiotti KE, *et al*. Identification of shared TCR sequences from T cells in human breast cancer using emulsion RT-PCR. *Proc Natl Acad Sci USA* 2016;113:8272–7.
26 Teng YHF, Quah HS, Suteja L, *et al*. Analysis of T cell receptor clonotypes in tumor microenvironment identifies shared cancer-type-specific signatures. *Cancer Immunol Immunother* 2022;71:989-98.